Supplementary Information

The *Toxoplasma* effector TEEGR promotes parasite persistence by modulating NF-kB signalling via EZH2

Laurence Braun[1], Marie-Pierre Brenier-Pinchart[1], Pierre-Mehdi Hammoudi[1], Dominique Cannella[1], Sylvie Kieffer-Jaquinod[2], Julien Vollaire[3], Véronique Josserand[3], Bastien Touquet[4], Yohann Couté[2], Isabelle Tardieux[4], Alexandre Bougdour[1]*, and Mohamed-Ali Hakimi[1] *

Supplementary Figures

A total of 10 supplementary figures are included here with legends.

Supplementary Tables

A total of 3 tables are submitted as separate SI Excel files and their legend are included here.

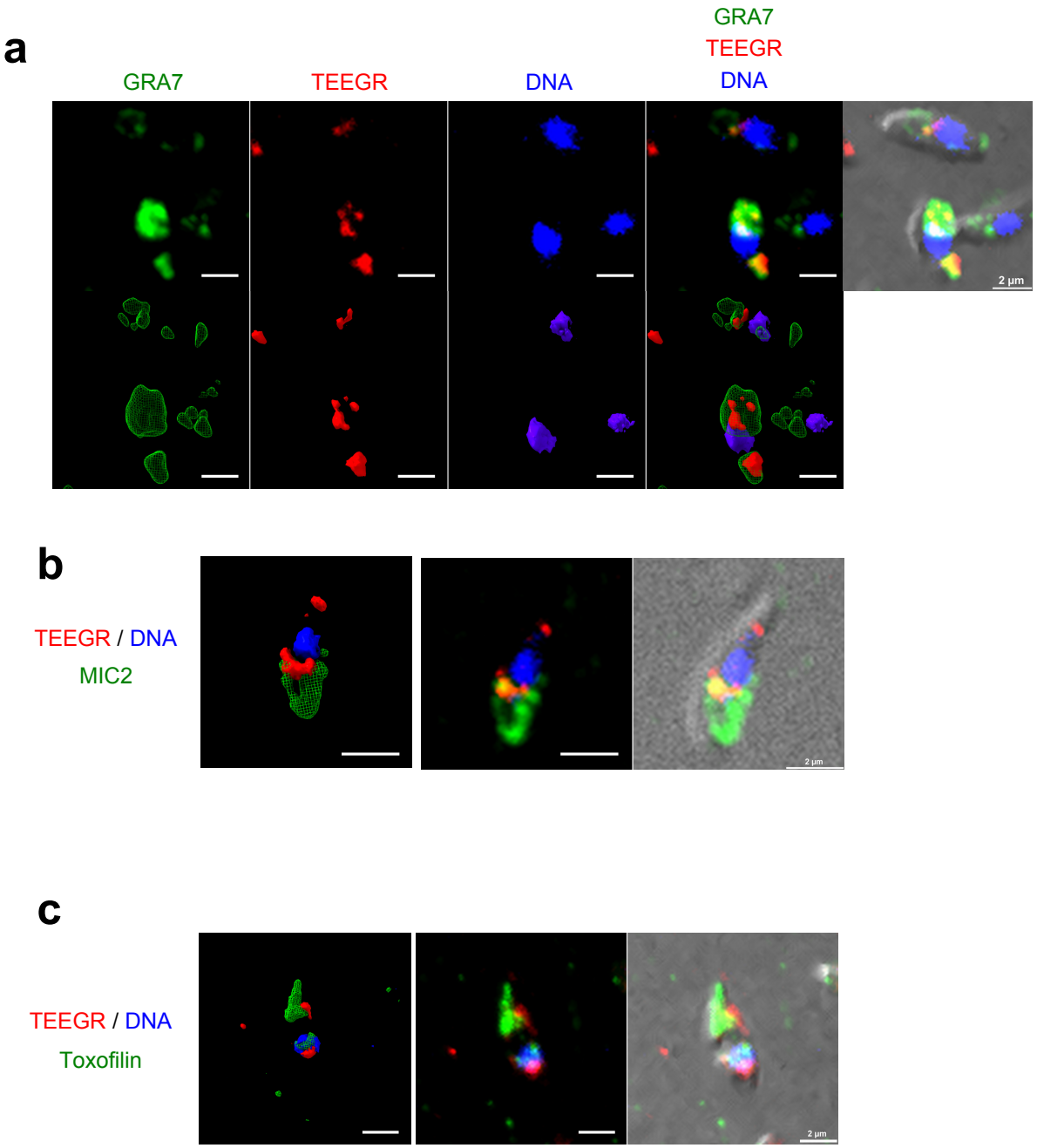

Supplementary Fig. 1

Supplementary Fig. 1 | TEEGR is a dense granule-resident protein. a-c, HAFlag (HF)-tagged TEEGR (in red) in PruΔ*ku80* extracellular parasites is contained in cytoplasmic organelles distinct from the apical micronemes (MIC2, in green) and rhoptries (Toxofilin, in green), and partially co-localizing with the dense granule protein GRA7 (in green). Cells were co-stained with Hoechst DNA-specific dye (in blue). Scale bars, 2 μm. All data are representative of 3 independent biological experiments (n=3).

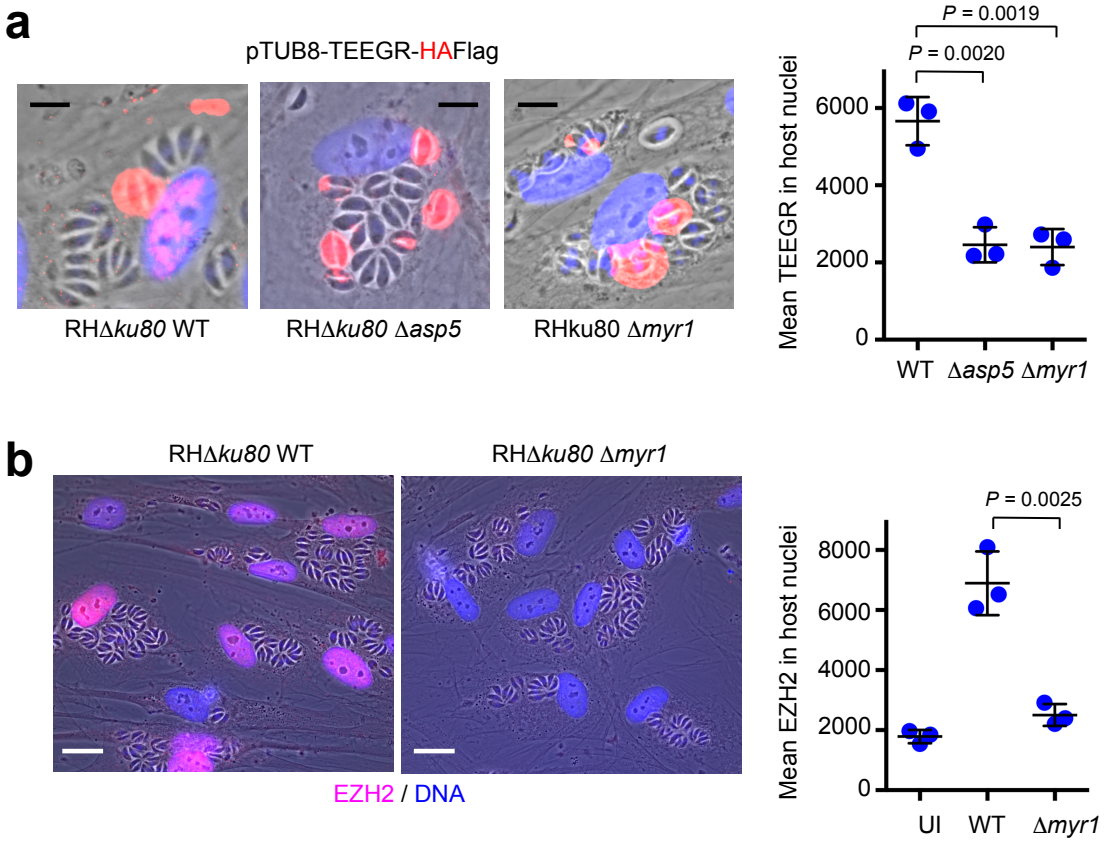

Supplementary Fig. 2

Supplementary Fig. 2 | The export of TEEGR in the host cell nucleus is mediated by ASP5 and MYR1. a, Representative IFA of WT, Δ*asp5* and Δ*myr1* parasites transiently expressing pTUB8-TEEGR-HAFlag (HA, in red). The amount of TEEGR in the nucleus was quantified in at least 100 host cells for each parasite strain. Horizontal bars represent the mean nuclear TEEGR intensity ± s.d. of three independent experiments (n=100 nuclei per dot). Scale bars, 10 μm. **b**, IFA of TEEGR-dependent induction of EZH2 (red) in infected HFFs (24 h) with WT and Δ*myr1* parasites. On the right, in situ quantification of nuclear EZH2 following infection. Horizontal bars represent the mean nuclear EZH2 intensity ± s.d. of three independent experiments (n=100 nuclei per dot). Scale bars, 20 μm. **c**, HFF cells were left uninfected (ui) or infected for 24 h with WT, Δ*teegr,* Δ*asp5* and Δ*myr1* strains from PruΔ*ku80* or RHΔ*ku80* genetic background. Levels of *iNOS* and *Alox12* mRNAs were determined by RT-qPCR. *β2*-microglobulin was used for normalization. Values were normalized to the amount of *β2*-microglobulin in each sample. Data are mean value ± SD of three replicates. The *p*-values were calculated using two-tailed unpaired Student's t-test, unless otherwise stated in the figure.

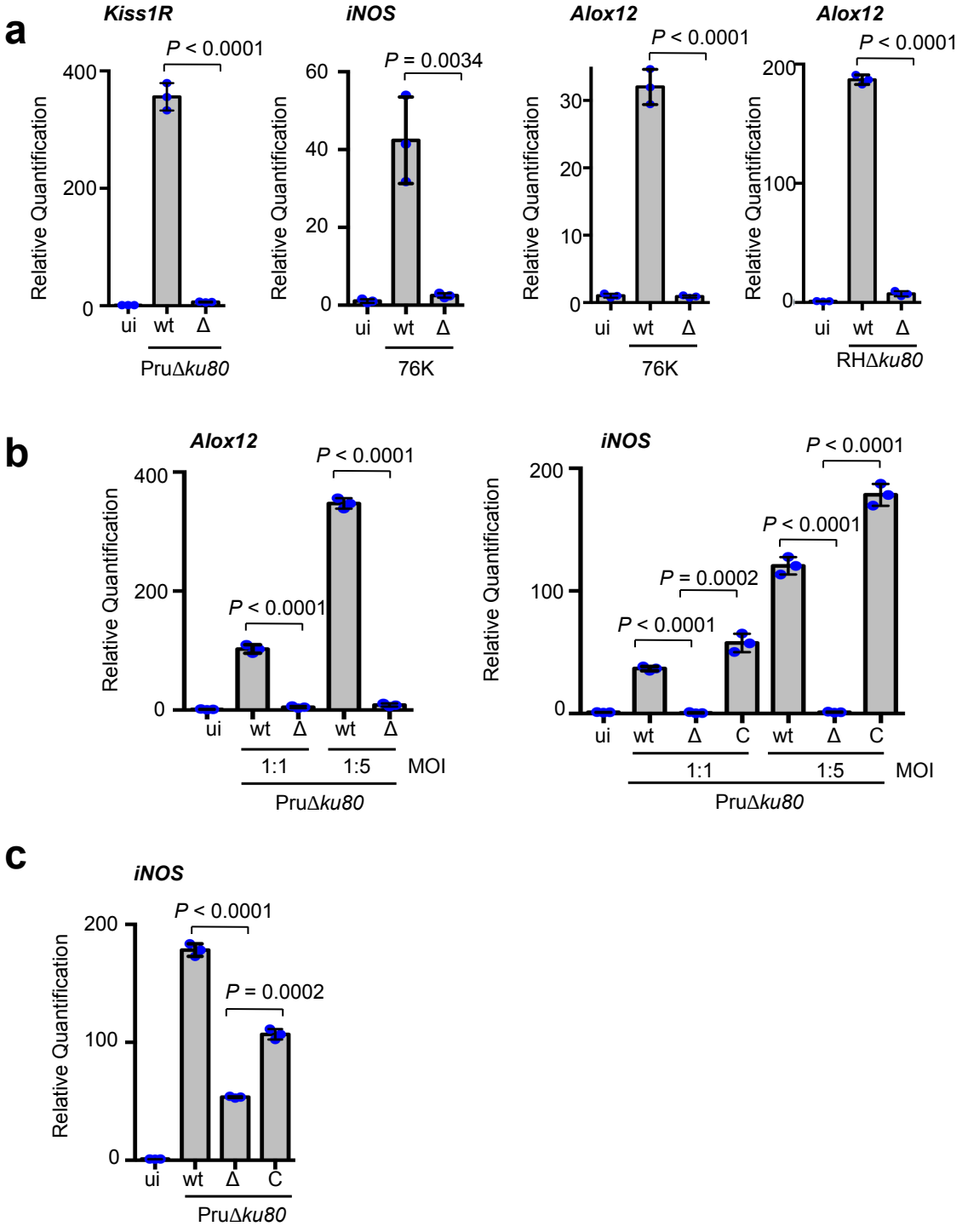

Supplementary Fig. 3

Supplementary Fig. 3 | TEEGR regulates positively the expression of *iNOS, Kiss1R and Alox12* in both human and murine cells. Human fibroblasts (**a**) or astrocytes (**b**) and murine Bone Marrow-Derived Macrophages (BMDM) (**c**) cells were left uninfected (ui) or infected with different multiplicity of infection (MOI) for 24 h with WT, Δ and C. Levels of *Alox12*, *Kiss1R* and *iNOS* mRNAs were determined by RT-qPCR. Values were normalized to the amount of $\beta 2$-microglobulin in each sample. Data are mean value ± SD of three replicates. The *p*-values were calculated using two-tailed unpaired Student's t-test, unless otherwise stated in the figure.

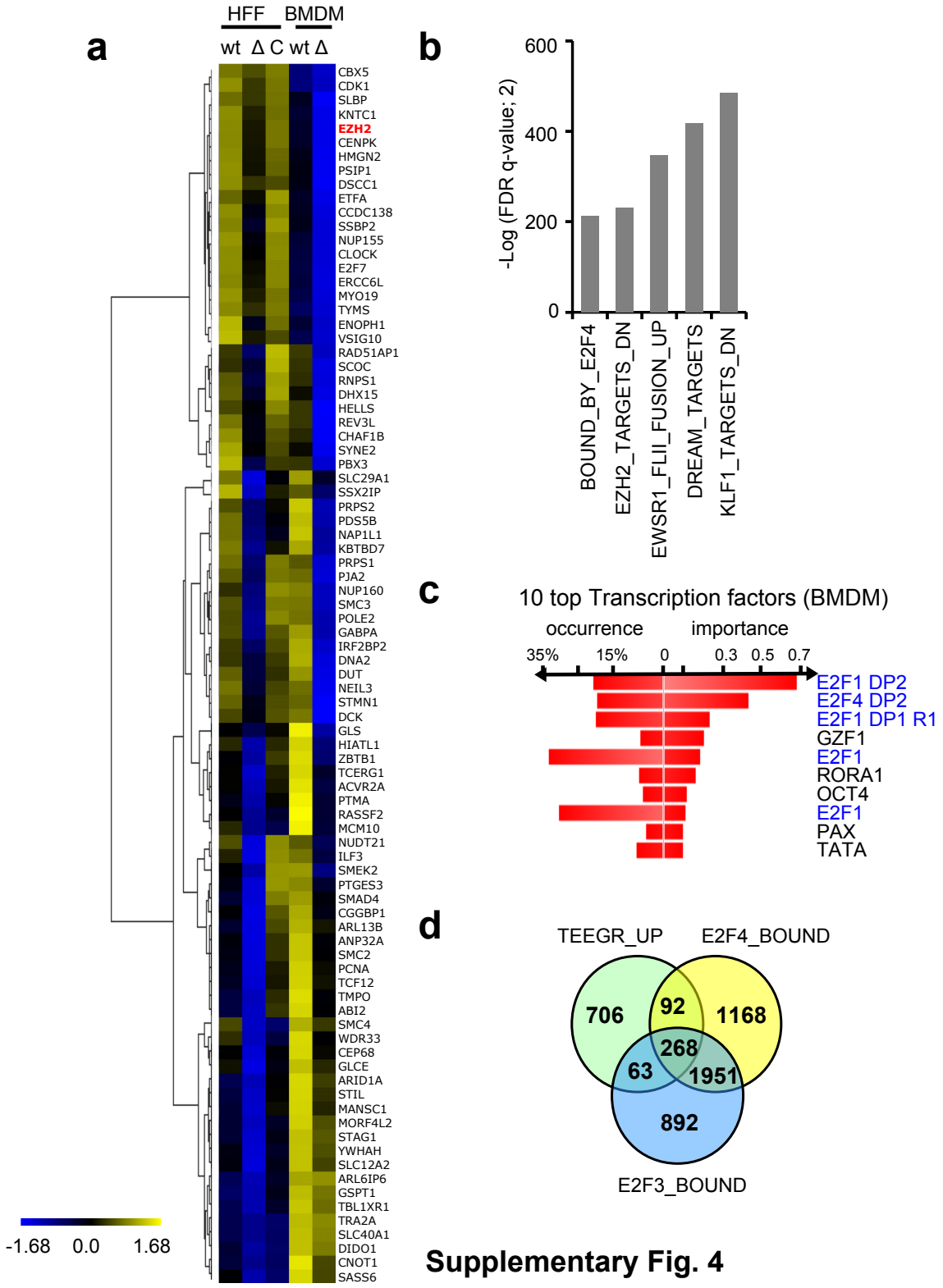

Supplementary Fig. 4

Supplementary Fig. 4 | TEEGR activates gene expression in murine macrophages in a E2F3 and E2F4-dependent manner. a, Heat map of expression values for differentially expressed genes in host cells infected with WT, Δ and C parasites. For the number genes (more than threefold, $P < 0.05$, unpaired t-test) that are defined as core TEEGR-regulated genes in HFF and bone marrow–derived macrophages (BMDM), mean log2 gene expression values were median centered, genes were clustered by hierarchical clustering based on Pearson correlation, and a heat map is presented. The complete set of genes is listed in GEO dataset (accession no. GSE113626). **b**, GSEA analysis of the 1129 genes positively regulated by TEEGR in BMDM highlighted five gene expression signatures of chemical and genetic perturbations (CGP) that were significantly and selectively enriched ($p < 0.05$, FDR-corrected, two-sided Welch t-test). **c**, TFBS analysis of the 1129 TEEGR-regulated genes was performed by DIRE and the most significant TFs are listed. **d**, Venn diagram illustrating the overlap between the number of genes up-regulated by TEEGR (> twofold, $p < 0.05$, unpaired t-test) in BMDM and the number of genes identified as E2F3- or E2F4-bound by Julian *et al*., (2016)[39] and Marson *et al*., (2007)[10], respectively.

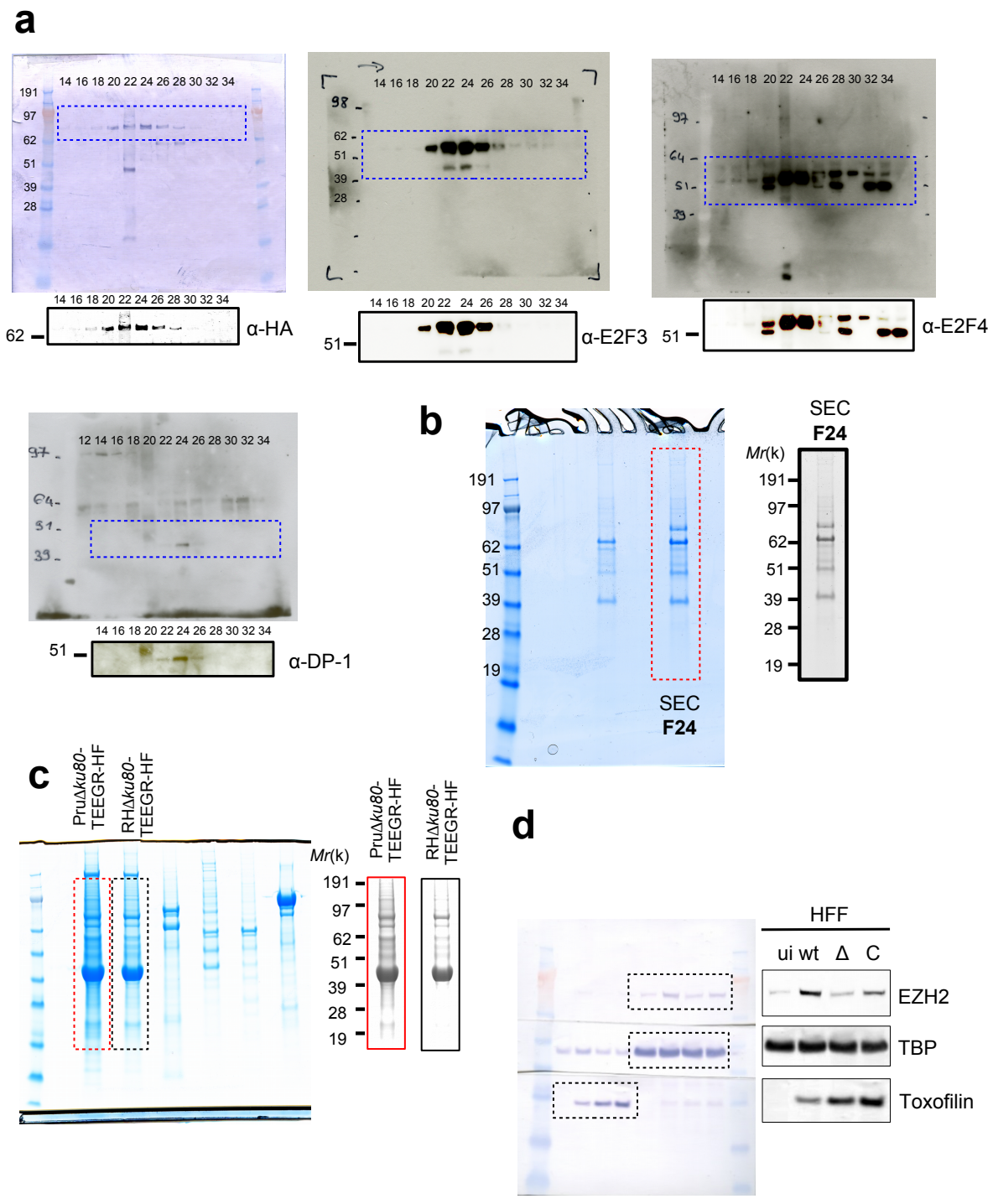

Supplementary Fig. 5

Supplementary Fig. 5 | Full blots for a, Figure 3b. **b**, Figure 3c. **c**, Figure 3d. **d**, Figure 4d. The dashed rectangles indicate the cropping zones.

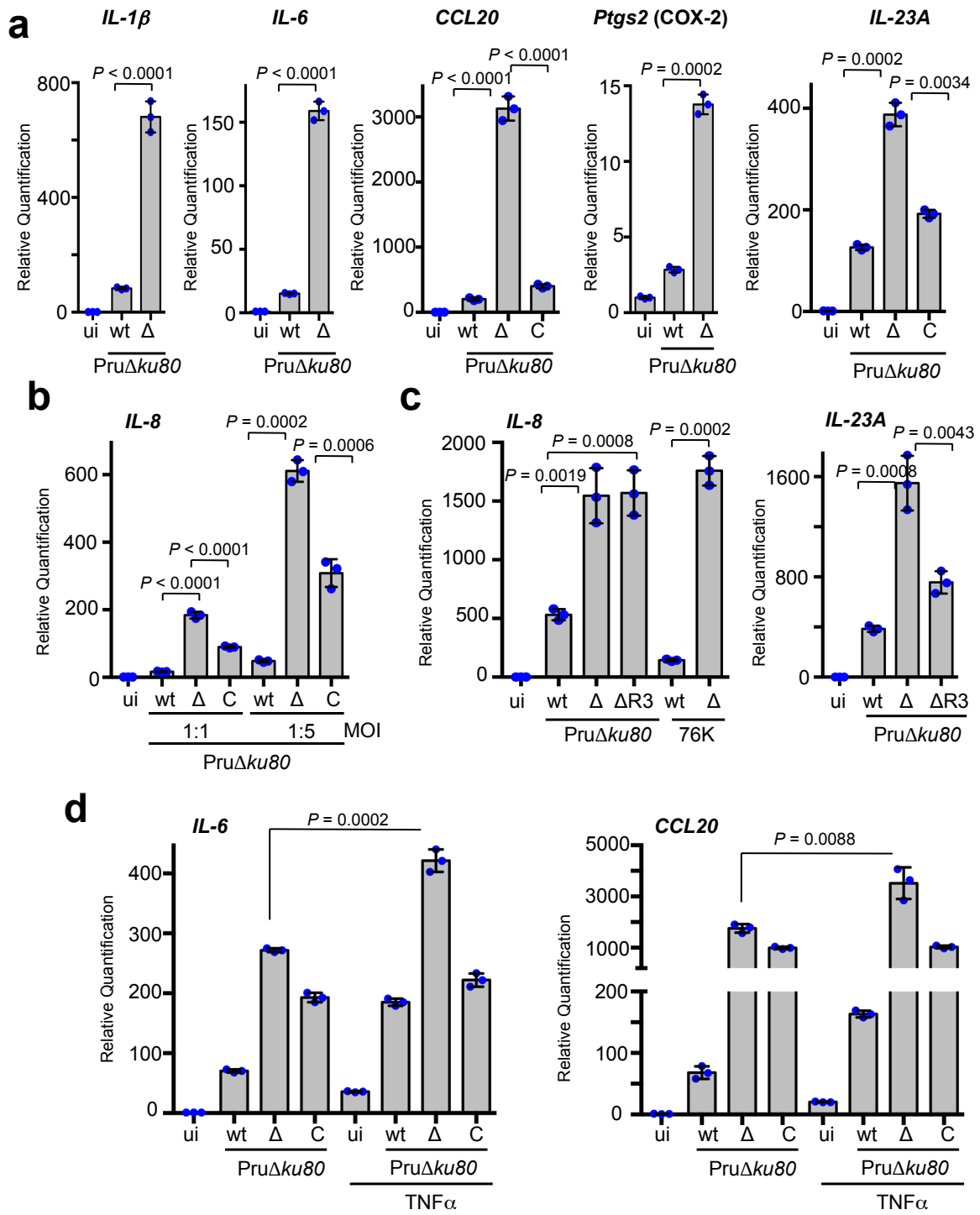

Supplementary Fig. 6

Supplementary Fig. 6 | TEEGR-dependent repression of *IL-1β*, *IL-6*, *IL-8*, *CCL20*, *IL-23A* and *Ptgs2* in human cells. a, Human astrocytes were left uninfected (ui) or infected for 24 h with WT, Δ or C strains. Levels of *IL-1β*, *IL-6*, *CCL20*, *Ptgs2* and *IL-23A* mRNA were determined by RT-qPCR. **b**, Human astrocytes were left uninfected (ui) or infected with for 24 h with WT, Δ and C strains with different multiplicity of infection (MOI). Levels of *IL-8* mRNA were determined by RT-qPCR. **c**, Human fibroblasts were left uninfected (ui) or infected for 24 h with WT, Δ and ΔR3 strains from type II (PruΔ*ku80* and 76K) lineages. Levels of *IL-8* and *IL-23A* mRNA were determined by RT-qPCR. **d**, Human fibroblasts were infected for 24 h with WT, Δ and C strains or left uninfected (ui) and stimulated for 6 h with TNF-α (50 ng/ml) or left unstimulated. Level of *IL-6* and *CCL20* mRNA were determined by RT-qPCR. (**a-d**) Values were normalized to the amount of *β2*-microglobulin in each sample. Data are mean value ± SD of three replicates. The *p*-values were calculated using two-tailed unpaired Student's t-test, unless otherwise stated in the figure.

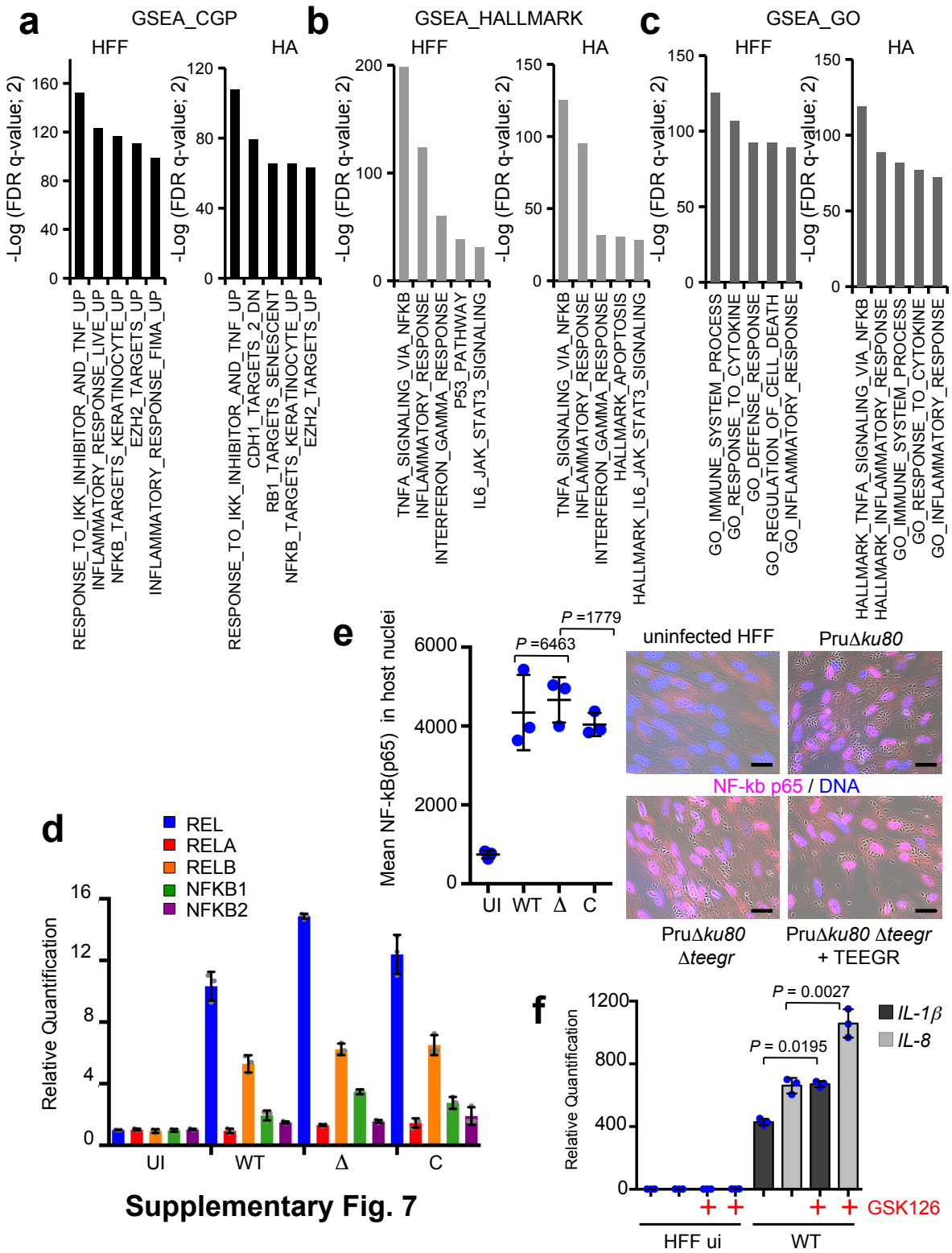

Supplementary Fig. 7

Supplementary Fig. 7 | TEEGR regulated negatively processes related to immunity. a-c, GSEA analysis of the 494 and 571 genes negatively regulated by TEEGR in HFF and HA cells respectively highlighted specific gene expression signatures of chemical and genetic perturbations (CGP), Hallmark and Gene Ontology (GO) that were significantly and selectively enriched ($p < 0.05$, FDR-corrected, two-sided Welch t-test). **d,** Human fibroblasts were left uninfected (ui) or infected for 24 h with Pru Δ*ku80* WT, Δ and C strains. Levels of NF-kB subunits mRNA were determined by RT-qPCR. Values were normalized to the amount of *β2*-microglobulin in each sample. Data are mean value ± SD of three replicates. **e,** Human fibroblasts were infected with *T. gondii* strains for 18 h, fixed, and stained with NF-kB p65 subunit (in red) and Hoechst DNA-specific dye (blue). Scale bars, 10 μ m. The amount of p65 in the nucleus was quantitated in at least 100 HFF cells for each strain. Horizontal bars represent the mean nuclear p65 intensity ± SD. An unpaired two-tailed Student's t-test indicated non-significant (ns) differences between the WT and Δ*teegr*. **f**, HFF cells were treated for 24 hours (+) with GSK126 or left untreated and infected for 24 hours with WT or left uninfected (ui). Levels of *IL-1β* and *IL-8* mRNA were determined by RT-qPCR. Values were normalized to the amount of *β2*-microglobulin in each sample. Data are mean value ± SD of three replicates. The *p*-values were calculated using two-tailed unpaired Student's t-test, unless otherwise stated in the figure.

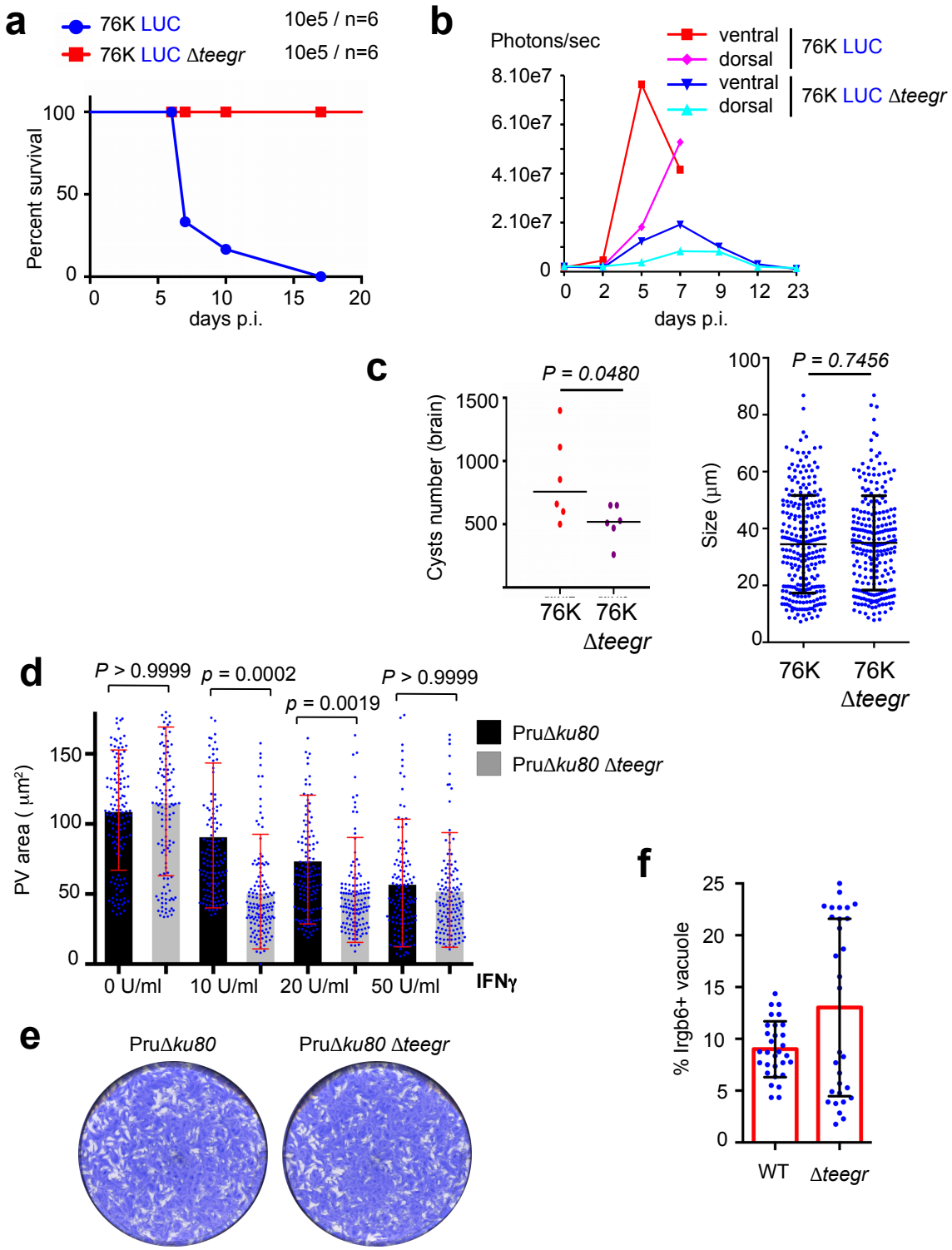

Supplementary Fig. 8

Supplementary Fig. 8 | Experiments comparing clearance of *Δteegr* to WT parasites *in vivo* in mice and in stimulated macrophages. a, Virulence of *Δteegr* strain was compared with its parental 76KGFP in BALB/c mice. Mice (n = 6) were inoculated with 10^5 tachyzoites by i.p. injection, and survival was monitored. Significance was tested using Log-rank (Mantel-Cox) test (*p*-value = 0.0161) and Gehan-Breslow-Wilcoxon test (*p*-value = 0.0154). A two-sided P value of <0.05 was considered statistically significant. **b**, Luminescent parasites were imaged with an IVIS imaging system from day 0 to 12 after the i.p. inoculation to BALB/c of 5.10^4 tachyzoites per condition. Graph depicts mean whole-animal radiance. **c**, Parasite burden in the brain BALB/c mice (n=6 animals/group) to which were given i.p a low dose (10^4) of 76KGFP or 76KGFP Δ*teegr* that allows both the parasite and host (<20 days) to switch to sustained parasitism through cysts that were enumerated using GFP parasites as a readout. The graph on the right shows the size of n=238 and n=258 cysts from wild-type or KO infections, respectively. Mean ± SEM. Significant p value < 0.05 (unpaired two-tailed Student's T-test). **d**, Mouse BMDMs were induced with 10, 20 or 50 U ml^{-1} of IFNγ for 24 h and infected with *T. gondii* WT or Δ*teegr* at an MOI of 0.5. Intracellular parasite growth was evaluated 24 h post-infection by determining the parasitophorous vacuole surface area (n=138 vacuoles per condition). Data are mean value ± SEM of three biological replicates. The *p*-values were calculated using one-way ANOVA. **e**, Parasites lacking *teegr* exhibit no growth defect in *vitro* in human fibroblasts by plaque assays. These experiments were repeated twice with similar results. **f**, Fluorescent signal intensities of Irgb6 protein was determined on coded slides. Data are mean value ± SD of two biological replicates. An unpaired two-tailed Student's t-test indicated non-significant differences between the WT and Δ*teegr* (n=140 vacuoles per condition).

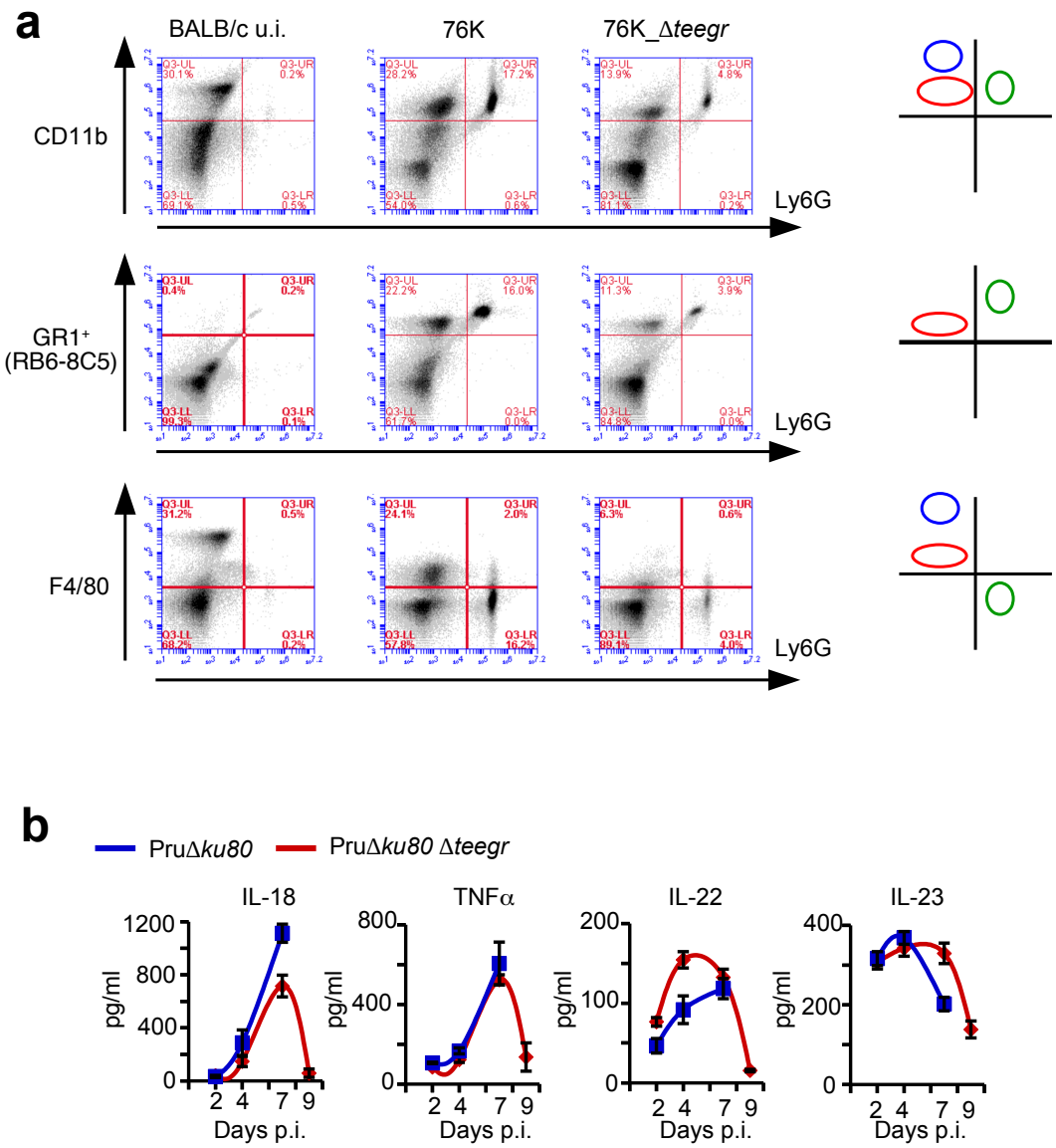

Supplementary Fig. 9

Supplementary Fig. 9 | Flow cytometry analyses of myeloid cells in the peritoneal lavage fluids after inoculation to mice of either WT or *teegr*-deficient parasites. a, Detection of resident peritoneal monocytes ($CD11b^+$ $Gr1^-$ $Ly6G^-$, blue circle), Gr1+ proinflammatory macrophages ($CD11b^+$ $Gr1^{int}$ $Ly6G^-$, red circle) and neutrophils ($CD11b^+$ $Gr1^{high}$ $Ly6G^+$, green circle) in the peritoneal lavage fluids of mice after *T. gondii* infection. Cell populations were characterized and quantified at day 4 p.i. by flow cytometry with anti-CD11b (conjugated to PE), anti-Ly6G (conjugated to APC), and anti-Gr1 (mAb RB6-8C5 conjugated to PE). Numbers indicate the percentage of cells within the gate. Results are representative of two or more independent experiments (n = 3 animals were pooled for each) for all panels. **b**, BALB/c mice were given i.p. a dose of 10^5 Pru*Δku80* or Pru*Δku80 Δteegr* tachyzoites. Peritoneal lavage fluids were collected on days 2, 5, 7, and 9 post inoculation. Number of tachyzoites was estimated within the collected samples by parasite DNA PCR and concentrations of IL-18, IL-22, IL-23 and TNF*α* were determined by ELISA. Data shown are means ± SD with n= 3 individual mice per parasite genotype at each time point.

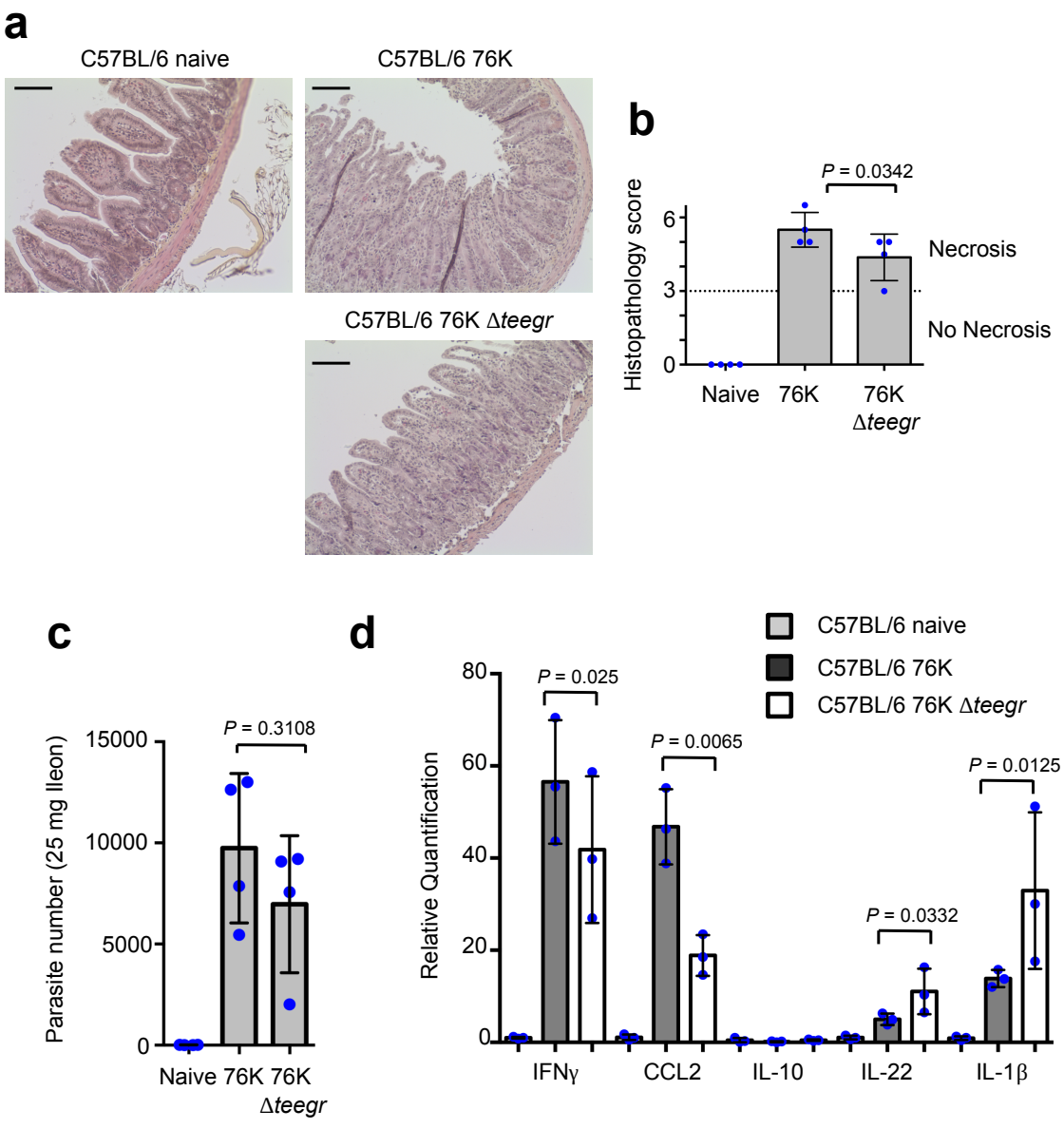

Supplementary Fig. 10

Supplementary Fig. 10 | Analysis of TEEGR phenotype in mice upon oral infection with *Δteegr* cysts. **a**, Histological analysis of ilea 8 days after cyst ingestion in C56BL/6 mice. Ilea of non-infected mice are characterized by a well-defined epithelial architecture and villous morphology. Mice infected with WT cysts are typified by a severe necrosis of the villi and mucosa compared to those challenged with *teegr*-deficient cysts. Bar, 100 μm. These experiments were repeated twice with similar results. **b**, Histopathological scores in the ilea of mice (n=4) infected with WT cysts were significantly lower compared with *teegr*-deficient-infected mice (n=4). Mean ± SEM. **c**, Parasitic load in ilea quantified by qPCR of C56BL/6 mice orally infected 8 days earlier. Statistical significance between Δ*teegr* and WT strains was tested by an unpaired two-tailed Student's t-test (Mann Whitney test). No significant difference was observed. **d**, qRT-PCR analysis of cytokines (IFNγ, IL-22, IL-10 and IL-1β) and chemokines (CCL2) in ilea of C56BL/6 mice orally infected 8 days earlier. RNA levels were normalized using TBP levels. Values were normalized to the amount of *β2*-microglobulin in each sample. Data are mean value ± SD of three replicates. The *p*-values were calculated using two-tailed unpaired Student's t-test, unless otherwise stated in the figure.

Table legends

Supplementary Table 1 | Differentially expressed genes between human cells infected with Pru Δ *ku80* and Pru Δ *ku80* Δ *teegr*. Sheet 1: Upregulated differentially expressed genes between Human Astrocytes infected with Pru*Δku80* and Pru*Δku80Δteegr* (n=784, fold change ≥2 and p value ≤0.05, unpaired t-test). **Sheet 2**: Downregulated differentially expressed genes between Human fibroblasts infected with Pru*Δku80* and Pru*Δku80Δteegr* (n=533, fold change ≥2 and p ≤0.05, unpaired t-test). **Sheet 3**: Upregulated differentially expressed genes between Human Astrocytes infected with Pru*Δku80* and Pru*Δku80Δteegr* (n=1529, fold change ≥2 and p ≤0.05, unpaired t-test). **Sheet 4**: Upregulated differentially expressed genes between Human Astrocytes infected with Pru*Δku80* and Pru*Δku80Δteegr* (n=629, fold change ≥2 and p ≤0.05, unpaired t-test). *P*-values were calculated from unpaired t-test. FDR is calculated from Benjamini Hochberg FDR.

Supplementary Table 2 | Differentially expressed genes between murine BMDMs infected with Pru Δ *ku80* and Pru Δ *ku80* Δ *teegr*. Sheet 1: Downregulated differentially expressed genes between BMDMs infected with Pru*Δku80* and Pru*Δku80Δteegr* (n=2376, fold change ≥2 and p value ≤0.05, unpaired t-test). **Sheet 2**: Upregulated differentially expressed genes between BMDMs infected with Pru*Δku80* and Pru*Δku80Δteegr* (n=2766, fold change ≥2 and p ≤0.05, unpaired t-test). *P*-values were calculated from unpaired t-test. FDR is calculated from Benjamini Hochberg FDR.

Supplementary Table 3 | Strains, Vectors and Primers. Sheet 1: List of *Toxoplasma* and mammalian cell lines as well as plasmids used in this work. **Sheet 2**: Primers and DNA synthesis construct used in this work.